The novel Solanum tuberosum *calcium dependent protein kinase, StCDPK3, is expressed in actively growing organs*

Carolina Grandellis, Verónica Giammaria, Magalí Bialer, Franco Santin, Tian Lin, David J. Hannapel & Rita M. Ulloa

Planta
An International Journal of Plant Biology

ISSN 0032-0935

Planta
DOI 10.1007/s00425-012-1732-9

Springer

Planta
DOI 10.1007/s00425-012-1732-9

ORIGINAL ARTICLE

The novel *Solanum tuberosum* calcium dependent protein kinase, StCDPK3, is expressed in actively growing organs

Carolina Grandellis · Verónica Giammaria · Magalí Bialer · Franco Santin · Tian Lin · David J. Hannapel · Rita M. Ulloa

Received: 24 May 2012 / Accepted: 30 July 2012

Abstract Calcium-dependent protein kinases (CDPKs) are key components of calcium regulated signaling cascades in plants. In this work, isoform StCDPK3 from *Solanum tuberosum* was studied and fully described. StCDPK3 encodes a 63 kDa protein with an N-terminal variable domain (NTV), rich in prolines and glutamines, which presents myristoylation and palmitoylation consensus sites and a PEST sequence indicative of rapid protein degradation. StCDPK3 gene (circa 11 kb) is localized in chromosome 3, shares the eight exons and seven introns structure with other isoforms from subgroup IIa and contains an additional intron in the 5′UTR region. StCDPK3 expression is ubiquitous being transcripts more abundant in early elongating stolons (ES), leaves and roots, however isoform specific antibodies only detected the protein in leaf particulate extracts. The recombinant 6xHis-StCDPK3 is an active kinase that differs in its kinetic parameters and calcium requirements from StCDPK1 and 2 isoforms. In vitro, StCDPK3 undergoes autophosphorylation regardless of the addition of calcium. The StCDPK3 promoter region (circa 1,800 bp) was subcloned by genome walking and fused to GUS. Light and ABRE responsive elements were identified in the promoter region as well as elements associated to expression in roots. StCDPK3 expression was enhanced by ABA while GA decreased it. Potato transgenic lines harboring StCDPK3 promoter::GUS construct were generated by *Agrobacterium tumefaciens* mediated plant transformation. Promoter activity was detected in leaves, root tips and branching points, early ES, tuber eyes and developing sprouts indicating that StCDPK3 is expressed in actively growing organs.

Keywords Calcium dependent protein kinases · Phytohormone responses · Signaling · *Solanum tuberosum*

Abbreviations

ABA	Abscisic acid
CDPK	Calcium dependent protein kinase
CaM	Calmodulin
NTV	N-terminal variable
2-DE	Two-dimensional gel electrophoresis
PGA	Polygalacturonic acid
GA3	Gibberellic acid

Introduction

Calcium ions are versatile signaling molecules in all eukaryotic organisms. In plants, spatially and temporally distinct "Ca^{2+} signatures" are evoked in response to different stimuli representing a central mechanistic principle to present defined stimulus-specific information. These specific "Ca^{2+} signatures" are formed by the tightly

Electronic supplementary material The online version of this article (doi:10.1007/s00425-012-1732-9) contains supplementary material, which is available to authorized users.

C. Grandellis · V. Giammaria · M. Bialer · F. Santin · R. M. Ulloa (✉)
Instituto de Investigaciones en Ingeniería Genética y Biología Molecular "Dr. Hector N. Torres", Consejo Nacional de Investigaciones Científicas y Técnicas, Vuelta de Obligado 2490 2° piso, C1428ADN Buenos Aires, Argentina
e-mail: rulloa@dna.uba.ar; ritaulloa@yahoo.com.ar

V. Giammaria · R. M. Ulloa
Facultad de Ciencias Exactas y Naturales, Universidad de Buenos Aires, Buenos Aires, Argentina

T. Lin · D. J. Hannapel
Plant Biology Major, 253 Horticulture Hall, Iowa State University, Ames, IA 50011-1100, USA

Published online: 25 August 2012

regulated activities of channels and transporters at different membranes and cell organelles (Dodd et al. 2010). The prototypical animal Ca^{2+} channels like the inositol (1,4,5)-triphosphate receptors appear to be absent from land plants, but were identified in the genomes of the evolutionary basal lineage of chlorophyta algae (Wheeler and Brownlee 2008). The loss of these channels in higher plants during evolution resulted in the development of "plant specific" Ca^{2+} signaling mechanisms which involved the adaptation of a "Ca^{2+} toolkit" at the level of the Ca^{2+} binding proteins that decode and transduce the information presented in Ca^{2+} signatures to downstream responses (Batistic and Kudla 2011). The information presented by a specific Ca^{2+} signal and its decoding by Ca^{2+} sensors represent the most critical step in specific information processing.

The Ca^{2+} toolkit in plants is formed by rather complex families of EF hand motifs Ca^{2+} sensor proteins that are represented by the calmodulin (CaM) and calmodulin-like protein (CML) family, the family of Ca^{2+} dependent protein kinases (CDPK), and the calcineurin B-like protein (CBL) family. These proteins exhibit Ca^{2+} dependent conformational changes upon Ca^{2+} binding. The genome of *Arabidopsis thaliana* encodes at least 250 EF hand proteins (Day et al. 2002). CaM is highly conserved in all eukaryotes, whereas CML, CDPK and CBL proteins appear to be specific to plants and lower protists (Harper and Harmon 2005; Wurzinger et al. 2011). CDPKs combine Ca^{2+} sensing (EF hand motifs) and a responding function (protein kinase activity) within a single protein and have therefore been classified as sensor responders (Harmon 2003). Consequently, these kinases translate information encoded in the Ca^{2+} signatures into phosphorylation events of specific target proteins.

Biochemical and molecular data help to gain insights into the subtle differences between members of the CDPK family, which in turn defines their specificity of action. Several studies derived from loss of function mutants and knocked down genes suggest that every CDPK isoform could have a distinct role such as stress response, oxidative stress, GA response, pollen tube growth and stomatal regulation (Ito et al. 2011). Moreover, CDPKs are targeted to multiple cellular locations (Dammann et al. 2003) suggesting that these proteins participate in various physiological processes including the accumulation of starch and proteins in immature rice seeds, tolerance to cold, salt and drought stress in Arabidopsis and rice (Mehlmer et al. 2010; Asano et al. 2011, 2012), defense response in tobacco (Romeis et al. 2000) and tomato (Chico et al. 2002), development and regulation of nodule number in *Medicago truncatula* (Gargantini et al. 2006), abscisic acid (ABA) response in Arabidopsis and pollen tube growth in petunia (Nakata et al. 2009).

Potato is one of the leading crops in sustaining the world's population due to the high nutritional value of its underground tubers (Navarro et al. 2011). Thus, it is of particular interest to understand the signaling pathways of potato that regulate developmental processes and stress responses to implement crop improvement. Tuber development is tightly controlled and both external and internal factors trigger this process; among them calcium and protein kinases play an important role (Balamani et al. 1986; Raíces et al. 2003a). Our group has studied the stolon to tuber transition in potato plants focusing on CDPK isoforms that are expressed in tuberizing stolons (Raíces et al. 2003b). StCDPK1 and StCDPK2 have been previously characterized. StCDPK1 plays a role in GA signaling and could influence tuberization (Gargantini et al. 2009), whereas StCDPK2 is associated with plant growth and development and its expression is highly regulated (Giammaria et al. 2011).

In the present study, the expression and activity of isoform StCDPK3 is described. The expression profile under different conditions shows ABA as a positive regulator and GA as a negative regulator of its expression. *Stcdpk3* gene was studied and its promoter was fused to a glucuronidase (GUS) reporter gene and delivered into *Solanum tuberosum* leaf explants by *Agrobacterium tumefaciens*-mediated transformation. We show that StCDPK3 promoter is active in root tips, primary roots branches, leaves, tuberizing stolons, as well as in proliferating tissues from sprouts and axillary buds derived from in vitro grown tubers.

Materials and methods

Plant material

Virus-free tubers from *S. tuberosum*, L. var. *Spunta* (Diagnosticos Vegetales S.A., Mar del Plata, Argentina) were used for in vitro potato plants micropropagation. In vitro plants were micropropagated on a modified MS medium with the addition of 2 % (w/v) sucrose and 0.7 % (w/v) agar and maintained in a 16 h light photoperiod at 23 °C. Soil grown *S. tuberosum*, L. cv. *Spunta* potato plants were cultivated in a greenhouse under a regime of 16 h light (25 °C) and 8 h dark (20 °C).

Cloning of StCDPK3 coding sequence

The complete coding sequence was amplified using as template a cDNA library constructed from mRNA from stolons (kind gift of Salomé Prat, CNB-Cantoblanco, Madrid) and oligonucleotides that contains the ATG start codon of NtCDPK1 (St3-ATGfw AATGGGTGGTTGTTT TAGC) and a sequence derived from the 3′UTR region of

StCDPK3 (St3-UTRrev 5′-GTAGGTTGAATTCGCACG G-3′). The amplicon (~1,861 bp) was subcloned in pGEM®-T Easy (Promega) according to the manufacturer's instructions. Double-stranded phagemid DNA for automated sequencing was prepared with the QIAGEN Plasmid Midi Kit. Automated sequencing was performed by Macrogen Inc. (Seoul, Korea) using universal primers T7 and SP6. Assembly and analysis of DNA sequence data was completed using BLAST sequence similarity search (blast.ncbi.nlm.nih.gov/Blast). The coding sequence, 5′UTR and 3′UTR region (2,345 bp) was submitted to Genbank (Accession number: AF518003.2).

Cloning of StCDPK3 genomic sequence

BAC B15, that contains the StCDPK3 gene, was identified by screening a genomic library from the diploid potato clone HB171 (Giammaria et al. 2011). The BAC DNA was isolated and used as template for PCR reactions. Oligonucleotides were designed based on the predicted exons sequences and were used to amplify the missing intronic sequences. The amplified fragments were subcloned in pGEM-T Easy (Promega, Madison, WI, USA), sequenced (Macrogen Inc., Seoul, Korea) and assembled. Intron boundaries were identified using software to determine splicing sites. The complete genomic sequence (Accession JF308510) was submitted to GenBank.

In silico analysis

Analysis of StCDPK3 coding sequence was performed using the PredictProtein (http://predictprotein.org) website. Phosphorylation sites were predicted using NetPhos 2.0 software (http://www.cbs.dtu.dk/services/NetPhos/). StCDPK3 genomic sequence was blasted in http://potatogenomics.plantbiology.msu.edu/blast.html against *S. phureja* DM superscaffold (v3). Analysis of StCDPK3 promoter region was performed using PlantCARE (http://bioinformatics.psb.ugent.be/webtools/plantcare/html/) and PLACE (http://dna.affrc.go.jp/PLACE/). The following online available sites were used: ImageJ (Image processing and analysis in JAVA) http://rsbweb.nih.gov/ij/, Expasy SIB Bioinformatics Resource Portal http://expasy.org/, BLAST http://blast.ncbi.nlm.nih.gov/Blast.cgi Basic Local Alignment Search Tool, MEGA 4 Molecular Evolutionary Genetics Analysis http://www.megasoftware.net/, OligoCalc: Oligonucleotide Properties Calculator http://www.basic.northWestern.edu/biotools/oligocalc.html, ImageMaster 2D Platinum 7.0 (GE Healthcare).

Rapid amplification of cDNA ends (RACE 5′)

Total RNA from *S. tuberosum* ssp. *andigena* leaves was obtained and used for cDNA synthesis and as template for RACE 5′UTR assays. First strand RACE-ready cDNA was synthesized from the total RNA according to the First-Choice RLM-RACE kit protocol (Ambion Inc., Austin, TX, USA). The RACE-ready cDNA was used as template in a PCR with the kit-provided 5′ RACE inner primer and a StCDPK3 gene specific primer (GSP1: 5′-AGCAAGAAGT ATACCCAACAAGATGC-3′). Cycling conditions were as follows: 3 min at 94 °C; 4 cycles of 94 °C 45 s, 53.7 °C 45 s, 72 °C 1 min; 30 cycles of 94 °C 30 s, 53.7 °C 30 s, 72 °C 1 min; and 72 °C for 8 min. The RACE PCR products were visually examined on a 2 % agarose gels. This RACE PCR procedure produced one product of 239 bp upstream the ATG codon and was confirmed by sequencing at the DNA facility of Iowa State University (Iowa, USA).

Chromosome localization

Localization of StCDPK3 was conducted by co-segregation of single stranded conformation polymorphic (SSCP) DNA with RFLP and SSR markers of a framework map derived from two segregating populations BCB and BCT (Bonierbale et al. 1994; Feingold et al. 2005). Oligonucleotides amplifying both intronic and exonic regions were designed and PCR reactions were performed to identify polymorphic bands in BCB and BCT. Amplicons were electrophoresed in Mutation Detection Enhancement (MDE, Cambrex, Charles City, IA, USA) polyacrylamide gels. Mapping was performed using the Mapmanager QTX software (http://www.mapmanager.org). With the recent release of the complete potato genome by the Potato Genome Sequencing Consortium (PGSC; http://www.potatogenome.net) the localization was confirmed in silico.

RNA extraction

Total RNA was extracted from shoot apex, leaves, sprouts, stems, roots, tuberizing stolons and tubers from greenhouse plants and from in vitro control and treated plants. The plant material (0.1–1 g) was collected and ground in liquid nitrogen with mortar and pestle. Total RNA was obtained using the total RNA isolation, TRIzol reagent (Invitrogen, Carlsbad, CA, USA) or the RNeasy Plant Mini Kit (Qiagen Inc., Valencia, CA, USA) following the manufacturers' instructions. RNA was quantified using a Nanodrop 1000 (Thermo Scientific) and used for RT-PCRor Northern blots assays as specified.

Northern blot assays

20 μg of total RNAs from different tissues or control and treated plants were hybridized with a radiolabelled probe against the 3′UTR of StCDPK3 generated by random priming using the RadPrime DNA labelling system kit (Invitrogen) for PCR products. Blots were exposed to X-OMAT Kodak films. RNA loading was checked with EtBr staining. Hybridization conditions were the same as in Raíces et al. (2003b). Signal was scanned with a Phosphorimager Storm 830 (Amersham Pharmacia Biotech) and quantified with ImageQuant software.

StCDPKs recombinant proteins

The StCDPK3 (1,677 bp) and StCDPK1 (1,599 bp) coding regions were amplified using primers St3pENTRfw (5′-CCGGATCCCGATGGGTGGTTGTTTTAGC-3′) and St3pENTRrev (5′-GCGGCCGCCTAGAAAAGCTTTTGTTGTGGTTG-3′) and St1pENTRfw (5′-CCGGATCCGATGGGTGTTTGTTTGAGC-3′) and St1pENTRrev (5′-TTGCGGCCGCTTAGAAGAGCTTGCCTGGTTG-3′) that contained *Bam*HI and *Not*I restriction sites (underlined). The amplified fragments were digested with *Bam*H1 and *Not*1 restriction enzymes (Promega) and subcloned into Gateway pENTR2B Vector (Invitrogen). *Escherichia coli* DH5α transformants were subjected to kanamycin selection. The Gateway LR Clonase II Enzyme Mix kit was used to insert StCDPK3 or StCDPK1 coding sequences into the destination vector pDEST 17 (Invitrogen) via site specific recombination, thus obtaining the kinase proteins tagged with 6 consecutive histidine residues (6xHis) at the N terminus. *E. coli* BL21 codon plus transformants were selected with ampicillin and chloramphenicol. 6xHisStCDPK3 was efficiently produced after overnight induction of *E. coli* cells with 1 mM IPTG at 25 °C. When induction was performed at 37 °C, the recombinant protein was detected in the insoluble fraction of the bacterial extract. On the other hand, 6xHisStCDPK1 was produced after inducing *E. coli* cells with 1 mM IPTG during 2 h at 37 °C. Cells were harvested by centrifugation, resuspended in lysis buffer (50 mM NaH_2PO_4, 300 mM NaCl, 10 mM imidazole, pH 8) and incubated 30 min on ice with 1 mg mL^{-1} lysozyme. After sonication (6 cycles, 10 s each) at 4 °C, the lysate was centrifuged at 20,000 × *g* during 30 min. The supernatants containing the tagged proteins were purified by affinity chromatography using a nickel agarose column (Ni-NTA agarose, QIAGEN) according to manufacturer's procedures. A non-induced culture was used as negative control. The purification steps were analyzed by SDS-PAGE and Western blot with a monoclonal anti-His antibody (Sigma-Aldrich, St-Louis, MO, USA) and anti-StCDPK3 or anti-StCDPK1 specific antibodies. When performing phosphorylation assays, the purified recombinant proteins were dialyzed against 10 mM Tris HCl, pH 7.5, 200 mM EDTA for 2 h and then against 10 mM Tris HCl, pH 7.5. Kinase activity was missing when skipping this last step.

Protein kinase activity and autophosphorylation assays

CDPK activity was assayed according to Giammaria et al. (2011) in a reaction mixture containing 10 mM Tris–HCl, pH 7.8, 10 mM $MgCl_2$, 10 mM β-mercaptoethanol (BME), 10 μM [γ^{32}P]-ATP (specific activity 122 Bq $pmol^{-1}$, New England Nuclear) and 25 μM Syntide-2 (Sigma-Aldrich) with the addition of EGTA or $CaCl_2$ at indicated concentrations. Initial velocity (V_0) conditions were evaluated and kinetic parameters (apparent K_m and V_{max}) for Syntide-2 and ATP were obtained from double-reciprocal plots. Kinetic parameters were determined by averaging at least three independent activity assays.

The following inhibitors and CaM antagonist were used: 1 μM staurosporine (ST), 0.5–5 mM EGTA, 10 μg mL^{-1} compound 48/80, and 0.5 mM chloropromazine (CPZ). Several kinase substrates were assayed: the peptides (50 μM) Syntide-2 (PLARTLSVAGLPGKK), GS (PLSRTLSVAAKK) and CDPKS (PLSRTLSVSS) derived from glycogen synthase, Kemptide (LRRASLG) and Casein Kinase Substrate (CKIIS) (RRRADDSDDDDD) and the proteins (2 mg mL^{-1}): Myelin Basic Protein (MBP), Histone 1 (H1 Calf Thymus) and Histone IIA (HIIA) from Sigma-Aldrich.

Purified 6xHisStCDPK3 and 6xHisStCDPK1 were used for autophosphorylation assays in the presence of 1 mM EGTA or 20–50 μM $CaCl_2$, using the reaction mixture previously described in the absence of exogenous substrate and 5 μM [γ^{32}P]-ATP (specific activity 1,220 Bq $pmol^{-1}$, New England Nuclear). Reactions were stopped as described (Chico et al. 2002), analyzed on 12 % SDS-polyacrylamide gels that were transferred to nitrocellulose membranes and exposed to Kodak X-Omat films (Sigma-Aldrich) or signal was scanned with a Storm 820 Phosphorimager (Pharmacia-Biotech). Histone (H1) phosphorylation (0.1 mg mL^{-1}) was performed using the same conditions.

For two-dimensional gel electrophoresis (2-DE) the autophosphorylation reaction was conducted as follows: a reaction mix containing 20 mM Tris–HCl pH 7.5, 10 mM $MgCl_2$, 20 μM $CaCl_2$, 10 mM ATP, 10 mM BME, 10–100 μg 6xHisStCDPK3 was prepared and incubated during 1 h at 30 °C. The final reaction volume ranged among 100 and 300 μl (300 μl when preparative 2-DE were performed).

First and second dimension gel electrophoresis

Autophosphorylation reactions were precipitated during 12 h with 3 volumes of TCA buffer, 10 % acetone, 0.07 %

BME. Samples were centrifuged during 30 min at 10,000×*g*. Pellet was washed twice with 500 µl 100 % acetone, 0.07 % BME followed by 5 min centrifugation at 10,000×*g*, air dried and resuspended in isoelectric focusing (IEF) buffer containing 0.05 % (v/v) of immobilized pH gradient (IPG) buffer pH 4–7 (GE Healthcare), 0.001 % (w/v) bromophenol blue and 0.06 M DTT. Samples were incubated during 30 min at 37 °C, centrifuged for 15 min at 10,000×*g* and strip rehydration was performed by adding the samples to the plate where strips were placed. PlusOne Dry Strip Cover Fluid (GE Healthcare) was applied to cover the strips, followed by a 16–20 h incubation at 30 °C. Samples were first separated by IEF pH 4–7 non-linear (7 cm; GE Healthcare) according to the manufacturer's instructions. IEF strips were then transferred separately to an equilibration solution (6 M urea, 50 mM Tris base, 2 % (w/v) SDS, 26 % (v/v) glycerol 26 % (v/v), 0.001 % (w/v) bromophenol blue and 0.06 M DTT) and incubated for 15 min at room temperature. The strips were then transferred to the same solution omitting DTT but including 45 mg mL^{-1} iodoacetic acid and incubated for 15 min at room temperature.

After a brief rinse in 1.5 M Tris–HCl, 1 % SDS (pH 8.0), the strips were transferred horizontally onto 10 % (w/v) polyacrylamide gels and covered with 0.6 % (w/v) agarose, 0.001 % (w/v), bromophenol blue and 0.5 % SDS. Second dimension gels were run at 50 mA for 6 h. Proteins were visualized by colloidal Coomassie Brilliant Blue G-250 staining or proQ staining (Invitrogen). ProQ signal was detected in a Typhoon™ 9400 Variable Mode Imager (GE Healthcare). Prestained SDS-PAGE standards from Fermentas Life Sciences (Burlington, Canada) were used as molecular weight markers.

Western-blot assays

Western-blot analysis of protein samples (50 µg) was performed using an affinity purified polyclonal anti-StCDPK3 antibody (1:1,000, Genscript, http://www.genscript.com/) directed against an N-terminal peptide (H_2N-YTQQDAN GYRAGRG-$CONH_2$) present only in StCDPK3, a polyclonal anti-StCDPK1 antibody (1:300, Gargantini et al. 2009) or a commercial monoclonal anti-polyHistidine peroxidase conjugate antibody (1:5,000, Sigma). Anti-rabbit IgG coupled to peroxidase was used as secondary antibody for anti-StCDPK antibodies. Blots were developed with ECL reagent (Amersham Pharmacia Biotech, Uppsala, Sweden) according to the manufacturer's instructions.

Plant treatments

In vitro plants were grown during 3 weeks under multiplication conditions in MS medium with 2 % (w/v) sucrose. Plants were transferred for 24 h to liquid MS medium containing 2 % (w/v) sucrose and then for 0, 2 or 6 h to the same media with the addition (treatment) or not (control) of 5 µM Gibberelic acid 3 (GA) Sigma: G-1025, 10 µM ABA, 10 µM polygalacturonic acid (PGA) or 200 mM NaCl. Alternatively, in vitro plants were exposed to dark or cold (4 °C) conditions during 0, 2 and 6 h. Each treatment was repeated three times and five plants were used for each condition.

Semi quantitative RT-PCR

200 ng of total RNA from the tissue or whole plant (as indicated) was used for cDNA synthesis. M-MLV-Reverse Transcriptase (Promega) and random hexamers were used for reverse transcribing followed by DNase treatment and later inactivation. Control reactions to check equal amounts of cDNA were performed with specific oligonucleotides ubifw (5′-ATGCAGATCTTTGTGAAGAC-3′) and ubirev (5′-ACCACCACGGAGACGGAG-3′) to amplify a 250 bp Ubiquitin fragment (20 cycles, annealing temperature 55 °C) or 18Sfw (5′-ATGCAGATCTTTGTGAAGAC-3′) and 18Srev (5′-ACCACCACGGAGACGGAG-3′) to amplify a 101 bp fragment (24 cycles, annealing temperature 55 °C). PCR products were obtained by using specific oligonucleotides UTRfw (5′-CTTGCAACGAGCATAGAACG-3′) and UTRrev (5′-GTAGGTTGAATTCGCACGG-′3) to exclusively amplify a fragment of 164 bp corresponding to StCDPK3 3′UTR. Platinum Taq polymerase (Invitrogen) was used and the products were visualized in 1.4 % agarose gels. RT-PCR products were quantified using ImageJ software (Image processing and analysis in JAVA, http://rsbweb.nih.gov/ij/) and normalized using 18SrRNA or ubiquitin mRNA values.

Isolation and sequence analysis of the StCDPK3 promoter region

The Genome Walker Universal kit (Clontech Labs, Inc, Palo Alto, CA, USA) was used to isolate the promoter sequence of StCDPK3 gene according to the manufacturer's instructions. The gene specific primers were designed 15 bp downstream the ATG codon and named GSP1: 5′-AGCAAGAAGTATACCCAACAAGATGC-3′ for initial round of PCR reaction and GSP2: 5′-CCAGA AAGACCATATCAGGCCACCGC-3′ for nested PCR. The final PCR product of 1,841 bp was cloned into pGEM®-T Easy (Promega) via the TA cloning method and the construct sequence was confirmed by sequencing at the DNA Facility at Iowa State University. Coinciding alignments of the 5′UTR of StCDPK3 and the obtained sequence confirmed the isolation of the promoter region. The promoter was amplified using Platinum® Taq DNA

Polymerase High Fidelity (Invitrogen) and subcloned into the *Hin*dIII/*Bam*H site of the pBI101 binary vector (Clontech) containing the *β*-glucuronidase (GUS) reporter gene. The construct was confirmed by sequencing at the DNA facility at Iowa State University.

Transformation and plant regeneration

Three-week-old in vitro plants from *S. tuberosum* L. cv. *Desiree* were selected for transformation. Healthy leaves were excised and 2–3 cuts were made in the leaf blade of the adaxial side. Leaves were kept adaxial side down in infection medium (IM) in a Petri dish. About 60–70 leaves were prepared for each experiment. Each Petri dish was inoculated with 100 µl of Agrobacterium culture (OD = 0.8) and incubated for 15 min at room temperature with continuous shaking, sealed and kept in the dark for 48 h at room temperature. Then, leaves were placed adaxial side down in callus induction medium (CIM) and kept in a growth chamber with a 16 h light 8 h dark photoperiod for 1 week. Explants were then transferred to shoot induction medium (SIM) until shoot appeared. Once shoots reached a length of 1–2 cm they were transferred to rooting media (RM).

Media content

Infection medium (IM): phytohormone free MS salts and vitamins supplemented with 20 g L^{-1} sucrose.

Callus induction medium (CIM): MS salts and vitamins, 16 g L^{-1} glucose, 5 mg L^{-1} 1-naphthaleneacetic acid, Sigma: N-0640 (NAA), 0.1 mg L^{-1} 6-benzylaminopurine (BAP), Sigma: B-3408, 250 mg L^{-1}cefotaxime, 50 mg L^{-1} Kanamycin.

Shoot induction medium (SIM): MS salts and vitamins, 16 g L^{-1} glucose, 2.2 mg L^{-1}zeatin-riboside (ZR) Sigma: Z3541, 0.02 mg L^{-1} NAA, 0.15 mg L^{-1} GA3, 250 mg L^{-1} cefotaxime, 50 mg L^{-1} Kanamycin.

Rooting media (RM): MS salts and vitamins, 20 g L^{-1} sucrose, 250 mg L^{-1}cefotaxime, 50 mg L^{-1} Kanamycin.

Histochemical and fluorometric analyses

Expression of the *β-glucuronidase* (GUS) reporter gene was evaluated by incubating the tissue samples at 37 °C for 16 h in GUS buffer containing 1.0 M $NaHPO_4$, pH 7.0, 2 mM X-GLUC (5-bromo-4-chloro-3-indolyl-*β*-D-GlcUA). Samples were cleared with 70 % ethanol several times and photographed employing a Leica magnifying glass EZ4D.

In vitro tissue culture plants were homogenized using 500 µl of extraction buffer containing 100 mM sodium phosphate buffer, pH 7.0, 10 mM EDTA, 0.1 % sarcosine, 0.1 % Triton X-100, 10 mM BME. Samples were then centrifuged at 13,000 rpm for 30 min at 4 °C. The supernatant was recovered and protein quantification was performed by Bradford. Extracts containing approximately 10 µg of protein extract were diluted to 500 µl with extraction buffer containing 2.0 mM 4-methylumbelliferyl-beta-D-glucuronide (MUG) and incubated at 37 °C for 0, 1, 2 and 4 h. The reaction was stopped by adding 1.9 ml of 0.2 M Na_2CO_3. Relative fluorescence was measured using a fluorometer (FluroMax-2) with an excitation wavelength at 355 nm and an emission wavelength at 460 nm. The specific activity of GUS was calculated using a calibration curve for 4-methylumbelliferone.

Analytical methods

Protein determination was performed with the Bio-Rad Protein Assay reagent (Bio-Rad) using bovine serum albumin as standard.

Sequence data from this article can be found in the EMBL/GenBank data libraries under accession number(s): StCDPK1 AF115406, StCDPK3 AF518003, http://www.ncbi.nlm.nih.gov/nuccore/297342354, NtCDPK1 AF072908, StCDPK3 gene: JF308510.

Statistical analysis of the results

Data shown in blots or images where error bars are not indicated are representative of at least three experiments.

Results

StCDPK3 coding sequence analysis

Three clones encoding CDPK isoforms have been previously isolated from a potato stolon cDNA library (Raíces et al. 2003b). Among them, StCDPK3 was a partial ORF containing an incomplete catalytic kinase domain (from subdomain VIb onwards) and the autoinhibitory and regulatory domains. In order to amplify the missing coding sequence, a PCR approach was performed using another cDNA library from potato stolons as template. Assembly of ESTs and TCs performed in potato gene index database revealed that the partial clone was very similar (90 % homologous) to NtCDPK1 (AF072908). By using a forward 5′ primer designed based on NtCDPK1 amino terminus and a reverse primer designed on the non-coding UTR sequence of StCDPK3 we were able to obtain the full-length clone (AF518003, http://www.ncbi.nlm.nih.gov/nuccore/297342354).

The coding sequence was inserted into pGEMT-easy and sequenced revealing a 1,674 bp ORF. The deduced protein sequence is 558 amino acid residues long, with a predicted molecular mass of 63.3 kDa and a calculated pI

of 6.02. The predicted protein sequence contains the N and C-terminal variable domains (NTV and CTV), the kinase domain (KD), the autoinhibitory domain (A) and the regulatory CaM-like domain (CLD) with the four typical EF hand motifs. A prediction of protein structure from sequence information (http://www.predictprotein.org/) indicated that StCDPK3 secondary structure includes 34.2 % helix, 10.4 % strands and 55.4 % loops.

A phylogenetic analysis of the described potato StCDPK proteins was performed. Amino acid sequences of the five StCDPKs were compared with tomato (*S. lycopersicum*), rice (*Oryza sativa*), *A. thaliana* and tobacco (*Nicotiana tabacum)* CDPKs. These data were organized in a phylogenetic tree using the ME-boot of MEGA (Molecular Evolutionary Genetics Analysis, version 4.0) software and the neighbor-joining option (Fig. 1a). StCDPK3 BLAST alignments revealed high degree of identity with the coding sequences of LeCPK1 from tomato (AJ308296, Identities: 2,101/2,199 bp) and NtCDPK1 from tobacco (AF072908, Identities: 1,601/1,809). At the amino acid level, LeCPK1

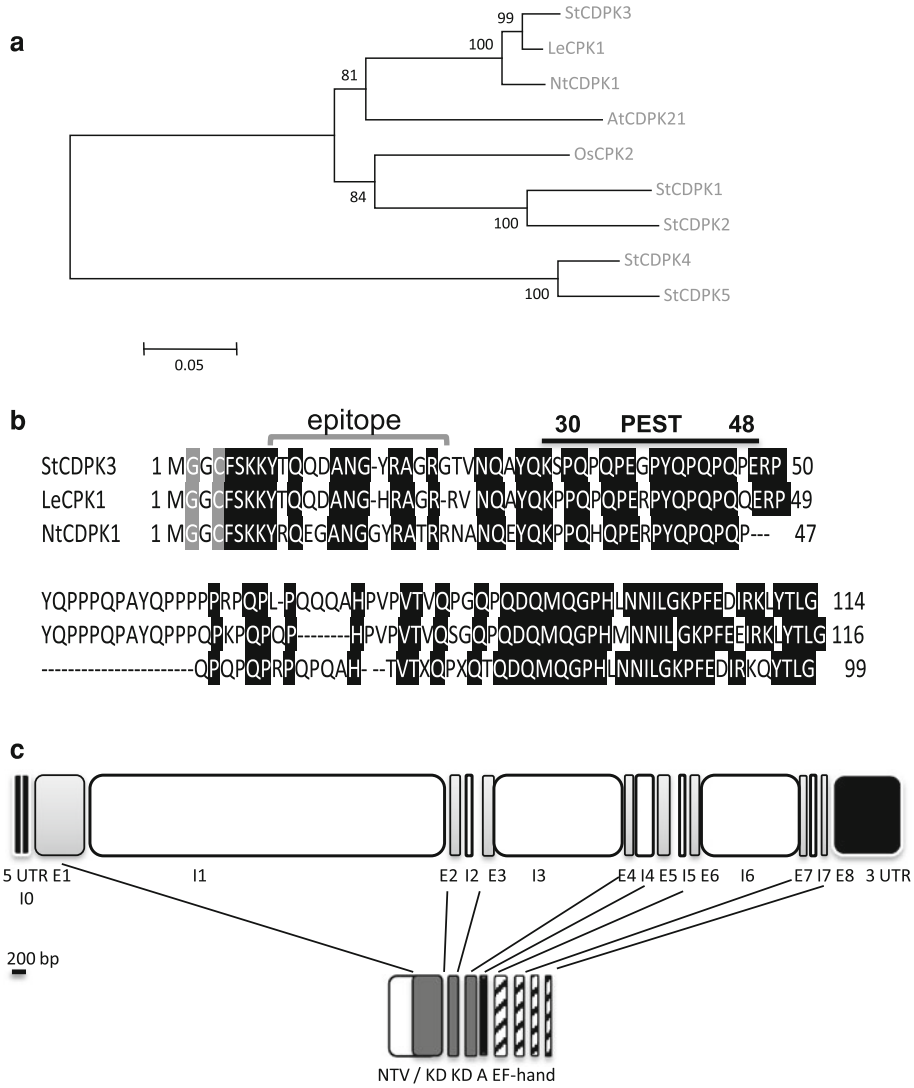

Fig. 1 **a** Phylogenetic tree of the StCDPKs described in *Solanum tuberosum*. The *numbers* shown in the branches are the boot-strapping values that indicate the level of significance (percentage) between two branches. The length of the *lines* in each branch indicates the degree of difference according to the provided scale in the *left side*. **b** Alignments of the N-terminal variable domains (NTVs) of StCDPK3, LeCPK1 from tomato and NtCDPK1 from tobacco. Identical residues are shaded in *black* and the glycine (G) in position 2 and the cysteine (C) in position 4 are shaded in *grey*. The PEST sequence is indicated. A *grey line* indicates the NTV peptide used as antigen to obtain the anti-StCDPK3 antibody. **c** Scaled scheme of *StCDPK3* gene structure and coding sequence (CDS). Untranslated regions (UTRs) are shown in *black*, introns (I) in *white* and exons (E) in *grey*. In the coding sequence, CDPK domains are indicated as follows: *NTV* N terminal variable domain (encoded by exon 1: 1–345 bp), *KD* kinase domain (encoded by exons 1: 346–795 bp, 2 and 3), *A* autoinhibitory domain (encoded by exon 4), *R* regulatory domain containing 4 EF hand motifs CaM-like (encoded by exons 5–8). The *bar* indicated corresponds to 200 bp

and NtCDPK1 share 95 and 88 % identity with StCDPK3, respectively and even when comparing the NTV domains, they are very similar (Fig. 1b) and cluster together in the tree (Fig. 1a). LeCPK1 and StCDPK3 share a 16 amino acid track that is missing in NtCDPK1, while StCDPK3 and NtCDPK1 conserve four amino acids (QQQA and QPQA, respectively) that are absent in the tomato isoform (Fig. 1b).

The NTV domain of StCDPK3 presents a long contiguous segment with non-regular secondary structure (NORS region, between amino acids 1 and 120); contains a predicted PEST sequence (score 8.3) in position 30 that is usually associated with rapid protein turnover followed by a low complexity region (amino acids 32–93) that is rich in prolines and glutamines (representing 36 % of the amino acids present) and predicted protein–protein interaction sites at positions 29–30, 48 and 60. As with many other CDPKs, StCDPK3 contains a Gly residue at position 2 and a Cys residue at position 4 that are potential conserved myristoylation and palmitoylation sites (Fig. 1b). According to Schlessinger et al. (2007) the structural plasticity of proteins with unstructured regions may facilitate its binding to many proteins, i.e., may typify a protein–protein interaction hub.

The comparison with the potato isoforms revealed that StCDPK3 shares the highest identity with StCDPK1 (75 %) and StCDPK2 (74 %); the three belong to the same subgroup (II-a) of the CDPK family. StCDPK4 (65 %) and StCDPK5 (59 %) are more distantly related, clustering together in a separate branch of the tree. When compared with the 34 Arabidopsis and the 31 rice CDPK isoforms, StCDPK3 shares the highest identity with AtCPK21, recently identified as a regulator of the guard cell anion channel SLAC1 (Geiger et al. 2010) and with OsCPK2 that is dominantly expressed in the panicle and the stamen (Ye et al. 2009).

Gene structure and chromosome localization

The complete gene sequence spanning 11.02 kb was amplified using a PCR-based technique. Introns were amplified using oligonucleotides designed on the exonic regions; genomic DNA or BAC B15 containing the *StCdpk3* gene were used as template. Splicing sites were identified and intron length was determined (Table 1;

Table 1 *StCdpk3* gene structure description (a) and gene environment (b)

StCDPK3 gene structure[a]					
Exons	bp	GC%	Introns	bp	GC%
5 UTR	239	36	Intron 0	350	
Exon 1	794	44.6	Intron 1	4,427	31.9
Exon 2	142	44.4	Intron 2	88	36.4
Exon 3	154	39	Intron 3	1,816	35.2
Exon 4	115	45.2	Intron 4	254	36.2
Exon 5	167	43.7	Intron 5	76	34.2
Exon 6	127	38.6	Intron 6	1,379	36
Exon 7	101	43.6	Intron 7	80	35
Exon 8	77	41.6			
3 UTR	984	32.8			

Identity	Gene name	Orientation
Upstream		
PGSC0003DMG400005052	Disease resistance protein RGA	→
PGSC0003DMG400005076	Conserved gene of unknown function	←
StCdpk3 gene ←[b]		
Downstream		
PGSC0003DMG400005078	Conserved gene of unknown function	←
PGSC0003DMG40105053	Uncharacterized GP1-anchored protein	→
PGSC0003DMG402005053	Gene of unknown function	ND
PGSC0003DMG400005079	RNA polymerase	←

[a] The length of untranslated regions (UTRs), introns and exons (in bp) and GC% content is shown

[b] Genes surrounding *StCdpk3* gene in the region between 829,650 and 869,649 bp of superscaffold PGSC0003DMB000000039 are listed. The arrows indicate genes' orientation. Gene identity is based in homology to *Arabidopsis thaliana* database (TAIR). Accession numbers are indicated

Fig. 1c). *StCdpk3* follows the eight exons/seven introns pattern present in *StCdpk1* and *StCdpk2* and the length of exons 2–7 is conserved varying only in a few nucleotides (Gargantini et al. 2009; Giammaria et al. 2011). However, *StCdpk3* contains an unusually large intron 1, and introns 3 and 6 are significantly larger than those present in *StCdpk1* and *2* genes. The total intronic content of the gene represents 82.8 % of the full sequence. The average GC content in introns is 34.9 %, while in exons the average is 40.9 %. In addition, this gene contains an intron in the 5′UTR region. The +1 transcription start site (TSS) was determined by RACE 5′ assay and this region comprises 593 bp followed by the ATG codon. A 350 bp intron was identified when the genomic sequence and sequences from the RACE 5′ products were overlapped. This intron was designated intron zero (I_0) and contains the consensus splicing sites AG in the 5′ end and GT in the 3′ end, and a 30.3 % GC content.

To define the chromosome location of *StCdpk3,* mapping experiments were performed using amplicons derived from intronic and exonic regions of the gene using the SSCP technique. Two polymorphic bands were observed in BCT segregating population (one from each parental genotype). Co-segregation analysis of these bands with pre-existing markers of both BCT_H and BCT_M maps localized *StCDPK3* in chromosome 3 (data not shown). The public release of the potato genome sequence (PGSC) allowed us to identify *StCdpk3* in the superscaffold PGSC0003DMB000000039 that belongs to chromosome 3, further verifying the previous localization assay. An in silico search was performed to find genes located up and downstream of *StCdpk3* (Table 1). *StCdpk3* is flanked upstream by a gene coding for a disease resistance protein RGA and also by a conserved gene of unknown function. Downstream it is flanked by a conserved gene of unknown function, a gene coding for an uncharacterized GPI-anchored protein, a gene of unknown function and a RNA polymerase.

Expression analysis of StCDPK3 in potato plants

To determine the expression profile of StCDPK3, different plant tissues and organs were analyzed by semi-quantitative RT-PCR and Northern blot. Total RNA was extracted from soil-grown plants from *S. tuberosum*, L. var. *Spunta* and Northern blot revealed that *StCDPK3* transcripts are present in aerial tissues such as leaves and sprouts, as well as in underground tissues such as roots and tubers (Fig. 2a, right panel). Tuber development comprises tuber initiation, tuber bulking and tuber maturation. Under appropriate conditions, the tips of underground elongating stolons (ES) hook and begin to swell (early induced stolons, EIS) resulting in initiation of new tubers that are not appreciably enlarging. At this stage (EIS), enhanced accumulation of *StCDPK3* mRNA was observed, but once stolon swelling was evident (Sw) with radial growth and accumulation of water, starch and nutrients, transcript abundance decreased (Fig. 2a, left panel). These results are consistent with previous reports showing that *StCDPK3* is transiently expressed in early stolons and its expression declines upon stolon swelling (Raíces et al. 2003b). RT-PCR was also performed in various tissues of *S. tuberosum* ssp. *andigena* plants that require a short-day (SD) photoperiod for tuberization. *StCDPK3* transcripts were detected in shoot apex, short and long day leaves, short and long day petioles, roots and stolons indicating that it is ubiquitously expressed (data not shown).

In order to evaluate StCDPK3 protein levels in extracts from the different organs in which expression was observed, a specific antibody was produced against a 14 amino acid stretch present at the NTV domain of the protein (indicated in Fig. 1b). Though the antibody specifically recognized the recombinant 6xHisStCDPK3 protein, we only detected StCDPK3 protein in the particulate fraction of leaf extracts (Fig. 3b, right panel) indicative of an association with cellular membranes, which is consistent with the presence of potential myristoylation and palmitoylation sites in G2 and C4. No signal was observed in other tissues tested (Fig. 3b, left panel) probably due to low expression levels or rapid protein degradation, maybe related to the PEST sequence present in its NTV domain.

6xHisStCDPK3 recombinant protein is an active CDPK

According to our expression results StCDPK3 shares its tissue localization with other CDPK isoforms. Our previous studies showed that StCDPK2 was detected in all the tissues analyzed though its expression was highest in leaves and sprouts exposed to light conditions (Giammaria et al. 2011), and that StCDPK1 was mainly expressed in tuberizing stolons together with StCDPK3 (Raíces et al. 2003b, c; Gargantini et al. 2009). The production of recombinant proteins is a useful tool to compare the biochemical parameters of different CDPK enzymes. As observed in Coomassie Brilliant Blue stained gels, 6xHisStCDPK3 was efficiently produced (Fig. 3a) and purified with a nickel agarose resin and the highest amount of recombinant protein was detected in eluent 2 (2.2 μg μL^{-1}) (E, Fig. 3b). These results were confirmed by Western blot using a monoclonal anti-His antibody (Fig. 3c, upper panel). CDPK activity was measured in the supernatant of induced and non-induced bacterial cultures; calcium dependent kinase activity was 3.5 fold higher in the induced culture verifying that the recombinant protein encodes an active kinase (data not shown). To further confirm the enzyme's identity, additional Western blots were performed using the

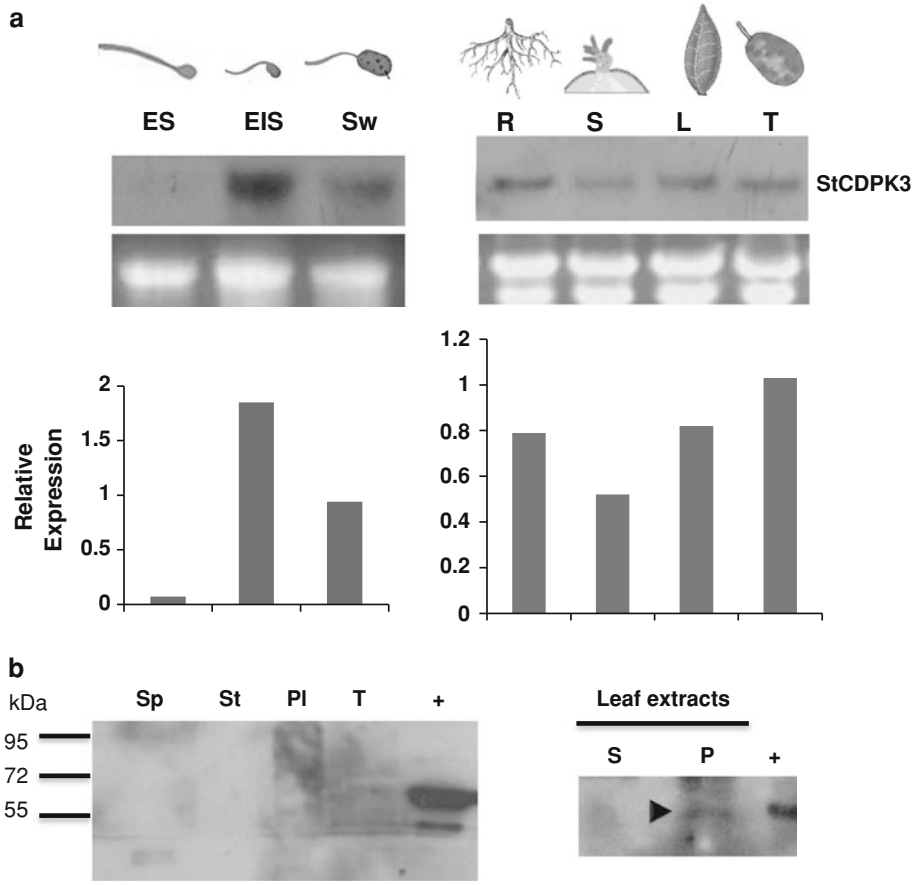

Fig. 2 Expression analysis of StCDPK3 in potato tissues. **a** Northern blot assays were carried out using 20 µg of total RNA from different tissues from *Solanum tuberosum*, var Spunta plants. *Left panel* elongated stolons (ES), early induced stolons (EIS) and swollen stolons (Sw). *Right panel* roots (R), sprouts (Sp), leaves (L) and tubers (T). Samples were electrophoresed on 1.4 % formaldehyde gels and blotted. Membranes were hybridized with a labeled dCTPαP^{32} probe spanning the 3′UTR of StCDPK3. Relative expression was calculated using ImageJ and rRNA 18S as loading control (represented as relative expression). **b** Western blot analysis. Anti-StCDPK3 antibody (1:1,000) was tested against the following plant protein extracts (40 µg): *Sp* sprouts, *St* stolons, *P* whole in vitro plant extracts, *T* tubers (*left panel*) and soluble (S) and particulate (P) fractions from greenhouse leaf extracts (*right panel*). Recombinant 6xHisStCDPK3 was used as positive control (+)

highly specific anti-StCDPK3 antibody that was able to recognize 6xHisStCDPK3 recombinant protein but not 6xHisStCDPK2 (Fig. 3c, lower panel). In parallel, the recombinant 6xHisStCDPK1 protein (60 kDa) was produced (inducing *E. coli* cells with 1 mM IPTG during 2 h at 37 °C) and purified with a nickel agarose resin (Fig. 3d). Its identity was confirmed using anti-StCDPK1 and anti-His antibodies (Fig. 3e). Anti-StCDPK3 was unable to detect this isoform (Fig. 3e).

Histone phosphorylation was assayed in gels using the recombinant proteins as enzyme source. Both isoforms, 1 and 3, can intensively phosphorylate H1 in a calcium dependent manner (Fig. 4); however, when recombinant StCPDK3 was tested, 1 mM EGTA reduced kinase activity but was unable to fully abolish it (Fig. 4a) while StCDPK1 activity was strongly reduced in its presence (Fig. 4b). In vitro autophosphorylation of CDPKs using recombinant or purified enzymes was observed for almost all CDPKs studied so far. Apart from the H1 band, a 63 or a 60 kDa band corresponding to the phosphorylated kinases was detected (Fig. 4). It is evident that autophosphorylation of StCDPK1 or StCDPK2 (Giammaria et al. 2011) was completely dependent on the presence of calcium; instead the recombinant StCDPK3 protein was also autophosphorylated in the presence of EGTA.

When no exogenous substrate was added to the assay, the phosphorylation of recombinant StCDPK3 was clearly enhanced (Fig. 4a); this could be the result of a competition with the substrate. The corresponding in vitro autophosphorylation sites (P-sites) have been mapped for several enzymes and were found with high frequency in the variable N termini (Witte et al. 2010). In silico searches for phosphorylation sites in the NTV region of both kinases were performed using the NetPhos 2.0 Server. While five

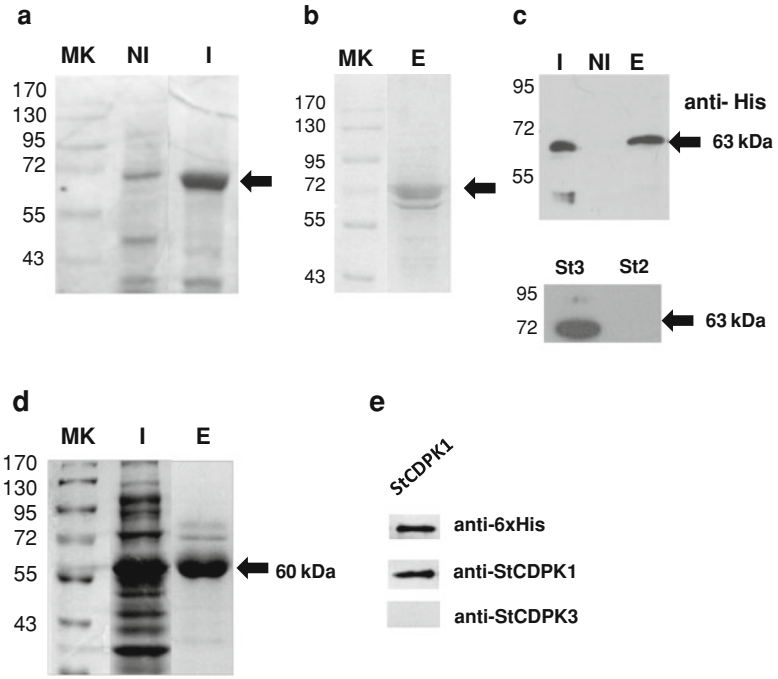

Fig. 3 **a** SDS-PAGE analysis of *E. coli* cell extracts (50 μg) containing the pDEST17-6xHisStCDPK3 vector induced (I) or not (NI) with 1 mM IPTG or **b** affinity purified recombinant protein (E, 200 ng). Both gels were stained with Coomassie Brilliant Blue. **c** Western blot analysis of I, NI and E using anti-His antibody (*upper panel*) or of purified recombinant 6xHisStCDPK3 and 2 proteins (St3 and St2) using anti-StCDPK3 antibody (*lower panel*). *Arrows* indicate the 63 kDa band corresponding to 6xHisStCDPK3. **d** SDS-PAGE analysis of IPTG induced *E. coli* cell extracts containing the pDEST17-6xHisStCDPK1 vector (I) and the affinity purified recombinant protein (E). Gels were stained with Coomassie Blue. **e** Western blot analysis of the purified 6xHisStCDPK1 with anti-His, anti-StCDPK1 and anti-StCDPK3 antibodies. *Arrow* indicate de 60 kDa recombinant protein. *Mk* molecular weight markers

serines (S) and one tyrosine (Y) sites were predicted in StCDPK1: S13 (score 0.997), S15 (score 0.839), S24 (score 0.814), S48 (score 0.851) and S62 (score 0.951) and Y19 (0.927); five tyrosines sites: Y9 (score 0.569), Y28 (score 0.529), Y40 (score 0.797), Y50 (score 0.806), Y58 (score 0.765) and one threonine site (T23, 0.669) were predicted in StCDPK3. This suggests that the different isoforms differ in their autophosphorylation requirements or in the potential upstream kinases that could target them and modulate their activity. Whether autophosphorylation is necessary to become activated remains to be elucidated, but clearly the phosphorylated kinases are active.

In order to study phosphorylation states for 6xHisSt CDPK3, the recombinant protein (100 μg) was subjected to an autophosphorylation assay in the presence of calcium and analyzed by 2-DE (Fig. 5). One gel was transferred to nitrocellulose and immunoblotted using an anti-His antibody; the signal detected in an estimated molecular weight range of 55–72 kDa spanned different isoelectric points (Fig. 5, upper panel). ProQ Diamond phosphoprotein stain of the second gel revealed that these spots correspond to different phosphorylation states of StCDPK3. Coomassie Brilliant Blue G-250 staining detected seven spots that could be extracted from the gel. A MALDI MS/MS analysis revealed that one of the spots matches a CDPK from *S. lycopersicum*, therefore confirming the identity of StCDPK3. These results indicate that StCDPK3 is phosphorylated in several residues generating a migration to the acidic region of the strip.

Biochemical and kinetics properties of 6xHisStCDPK3

The kinetic parameters, K_m and V_{max}, of both kinases were determined using Syntide-2 as acceptor substrate and ATP as donor substrate (Table 2). These values were estimated according to the double-reciprocal Lineweaver–Burk plot using the recombinant proteins as enzyme source. The results indicate that K_m for ATP and Syntide-2 are 3.3 μM and 31.2 μM, respectively for StCDPK3 and 19.7 μM and 7.8 μM, respectively for StCDPK1. As observed both kinases differ from StCDPK2 (Syntide-2 = 1.75 μM, ATP = 18 μM, Giammaria et al. 2011). It is evident that StCDPK3 displays the highest affinity for ATP. Both StCDPK1 and StCDPK3 reached a similar V_{max} (Table 2), however while StCDPK3 required 25 μM calcium to achieve its maximal phosphorylation capacity, StCDPK1 reached maximal activity at 2.5 μM calcium. On the other hand, 5 mM EGTA was required to completely abolish StCDPK3 kinase activity (data not shown) while 0.5 mM EGTA completely inhibited StCDPK1, demonstrating once

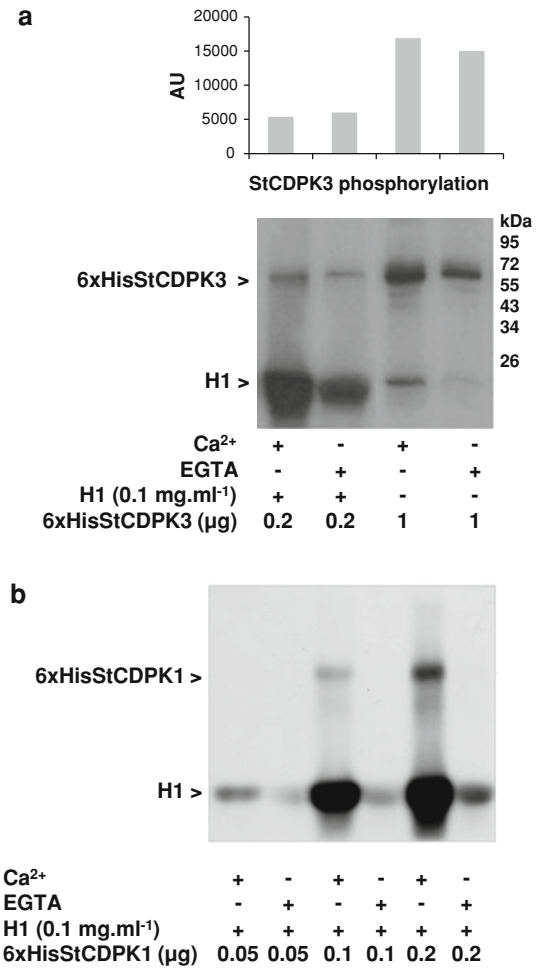

Fig. 4 Autophosphorylation and histone H1 phosphorylation. Kinase activity of 6xHisStCDPK3 (**a**) and 6xHisStCDPK1 (**b**) was assayed using 5 µM ATPγ^{32}P and analyzed by SDS-PAGE followed by autoradiography. Assays were performed in the presence of 20 µM Ca^{2+} or 1 mM EGTA. The enzyme concentration used in each lane is indicated. Molecular weight standards are shown on the *right* (kDa). StCDPK3 autophosphorylation signal was quantified using the ImageJ software and expressed in arbitrary units (AU)

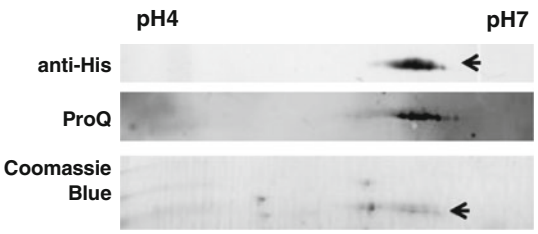

Fig. 5 Autophosphorylation of 6xHisStCDPK3 resolved by 2D gels. 6xHisStCDPK3 (100 µg) was incubated with ATP-Mg^{2+} during 1 h at 30 °C. **a** Western blot assays were revealed with anti-His antibody (1:5,000). *Arrow* indicates the spots corresponding to the 6xHisStCDPK3. **b** ProQ staining visualized with Typhoon™ 9400 Variable Mode Imager (GE Healthcare). **c** Coomassie Brilliant Blue staining

again that each isoform responds to its effectors and associates to its substrates in a particular way.

Further biochemical characterization was performed using the purified recombinant StCDPK3 protein (0.2 µg). The effect of inhibitors of kinase activity such as ST, the CaM antagonists, chlorpromazine (CPZ) and compound 48/80 and EGTA was evaluated. As shown in Fig. 6, CPZ completely abolished enzymatic activity and a similar effect was observed with compound 48/80. Staurosporine inhibits protein kinases by preventing ATP binding due to the stronger affinity of ST to the ATP-binding site on the kinase. The slight inhibition (25 %) observed with ST (Fig. 6a) could be due to the high affinity that this isoform displays for ATP. In the case of StCDPK1, ST reduced its activity to 50 % (data not shown). Different peptides and proteins were assessed as phosphate acceptors using the P81 assay. Among peptides, GS and Syntide-2 were the best substrates. Kinase activity was detected with CDPKS but StCDPK3 was unable to phosphorylate CKIIS and kemptide. When using proteins, MBP turned out to be the best phosphate acceptor (Fig. 6b).

Promoter isolation and in silico analysis

Using the Genome Walker Universal kit, the promoter sequence of *StCDPK3* was identified and amplified. A 1,942 bp fragment was obtained and inserted into the binary pBI101 vector and the promoter sequence was analyzed using the online available databases PlantCARE (http://bioinformatics.psb.ugent.be/webtools/plantcare/html/) and PLACE (http://www.dna.affrc.go.jp/PLACE/). A number of *cis*-acting elements described in other species were detected. Among them, is the 5′UTR Py-rich stretch (TTTCTTCTCT) at position 532 (−) described in *Lycopersicon esculentum* that is reported to confer high transcription levels, and two ABA-responsive element (ABRE) motifs, ACGTG and CACGTG, at positions 880 (−) and 439 (+) that were described in *A. thaliana* and are involved in ABA responsiveness (Table S1).

About 40 possible TATA boxes were detected; considering that this box is usually located 25–30 base pairs upstream of the TSS, we conclude that the sequence most likely to be the correct TATA box for TATA binding protein (TBP) binding is the site TATAAA located 54 bp upstream the TSS. As for the CCAAT box (a common *cis*-acting element in promoter and enhancer regions known to occur −165/−40 bp upstream the TSS) we observed that it was located 58 bp upstream the TSS overlapping the TATA box (CCAA**T**ATAAA). In addition, several light responsive elements reported in other plant species were detected all over the promoter region: CAG-motif 957 (+), G-box 439 (+), I-box 324 (−) and TCT-motif 142 (+), while numerous *cis*-acting regulatory elements involved in

Table 2 Biochemical parameters of isoforms StCDPK1, 2 and 3

CDPK isoform	ATP Donor substrate		Syntide-2 Acceptor substrate		Maximal activity
	K_m (μM)	V_{max} (μmol min^{-1} mg^{-1})	K_m (μM)	V_{max} (μmol min^{-1} mg^{-1})	Ca^{2+} (μM)
6xHisStCDPK1	19.7 ± 0.03	0.04 ± 0.005	7.74 ± 0.04	0.05 ± 0.01	2.5
6xHisStCDPK2[a]	18 ± 0.03	0.1 ± 0.007	1.75 ± 0.04	0.4 ± 0.05	0.6
6xHisStCDPK3	3.3 ± 0.02	0.033 ± 0.006	31.2 ± 0.04	0.094 ± 0.01	25

Values were estimated according to the double-reciprocal Lineweaver–Burk plot using the recombinant proteins as enzyme source. Calcium concentration required to reach maximal activity is indicated. Results are representative of three independent assays

[a] Giammaria et al. (2011)

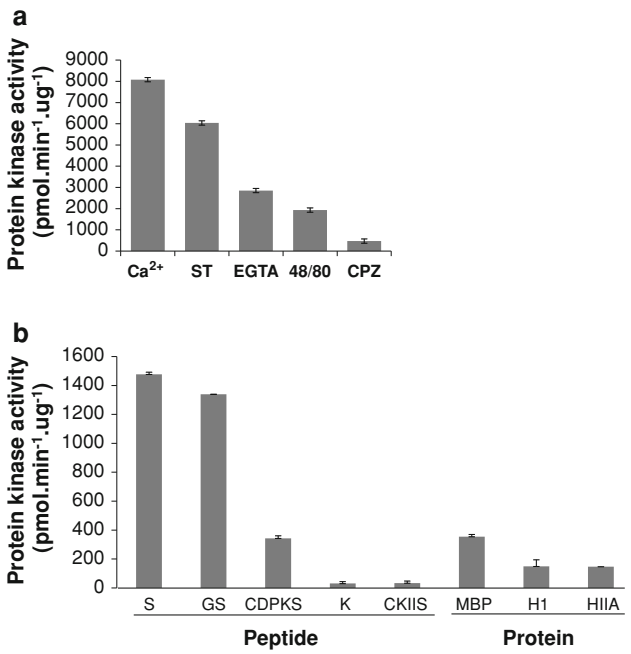

Fig. 6 Effect of inhibitors and antagonists on StCDPK3 activity and substrate preference analysis. **a** Specific CDPK activity was measured (pmol min^{-1} μg^{-1}) using Syntide-2 (25 μM) as phosphate acceptor and different inhibitors of kinase activity: 1 μM staurosporine (ST), 10 μg/ml compound 48/80, 0.5 mM chlorpromazine (CPZ) and 1 mM EGTA. **b** CDPK activity was measured (pmol min^{-1} mg^{-1}) using different synthetic peptides: Syntide-2 (S), GS, CDPKS (calmodulin dependent protein kinase substrate), CKIIS (casein kinase II substrate) and Kemptide (K) or proteins: HIIA (Histone IIA), H1 (Histone H1 calf thymus) and MBP (myelin basic protein) as phosphate acceptors

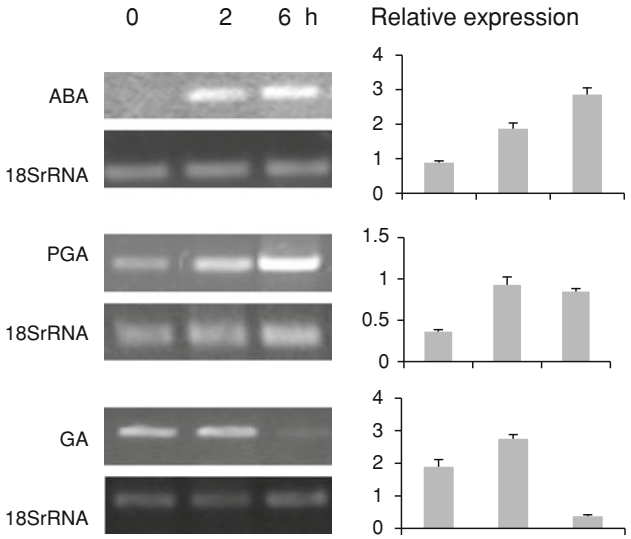

Fig. 7 StCDPK3 expression in response to hormone and stress treatments. In vitro grown plants were exposed to 10 μM ABA, 10 μM PGA and 5 μM GA3 treatments during 0, 2 and 6 h. RT-PCR analysis of StCDPK3 was performed and visualized. ImageJ software was used to normalize the expression levels to 18SrRNA levels and relative expression is shown. The experiments shown are representative of at least three experiments. *Error bars* are indicated

root-specific expression such as OSE1ROOTNODULE (AAAGAT), OSE2ROOTNODULE (CTCTT), ROOTMOTIFTAPOX1 (ATATT) and As1 (TGACGTCA) were repeatedly observed along the promoter (Table S1). These findings are in accordance with our Northern blot results (Fig. 2a) showing that StCDPK3 is expressed in roots.

Phytohormone and biotic stress responses

Based on the elements detected in silico in the promoter of *StCpdk3*, we decided to assay the effect of hormones (ABA and GA), cold, salt and darkness or the elicitor polygalacturonide (PGA) on *StCDPK3* expression using RNA from in vitro grown plants. The different treatments were performed for 2 or 6 h and expression of *StCDPK3* was analyzed by RT-PCR. StCDPK3 mRNA levels were up regulated in response to ABA and PGA, while phytohormone GA negatively modulated its expression (Fig. 7). *StCDPK3* expression increased threefold after 6 h of ABA treatment; on the contrary, it diminished almost fourfold after 6 h of GA treatment. No significant change in *StCDPK3* expression was observed when in vitro plants were exposed to cold, salt or dark conditions (data not shown). Thus, we conclude that the exogenously applied phytohormone ABA upregulated and that GA treatment decreased *StCDPK3* expression.

Analysis of transgenic lines carrying the StCDPK3 promoter fused to GUS gene

Transgenic potato plants carrying the *StCPK3* promoter fused to GUS were obtained (the construction is indicated in Fig. 8a). After kanamycin selection, thirteen lines were able to root in the media and were chosen for further analysis. Among them, eight lines were confirmed by PCR using oligonucleotides that amplify the *nos* gene and a fragment containing the partial promoter and the partial GUS coding sequence (Fig. 8b). These lines were further selected to measure GUS activity in fluorometric assays using MUG as substrate. Potato transgenic lines C, D, K and L showed high GUS activity compared to the wild type potato plants (Fig. 8c). In particular, lines C and L displayed the highest activity levels. Histochemical GUS staining was positive in C and L lines but not in K or M ones (Fig. 8d). Consequently, lines C and L were chosen for further expression profile characterization.

In vitro grown transgenic potato plants carrying the pStCDPK3-GUS construction showed promoter activity in leaves and roots and the pattern was common among the transgenic lines analyzed. Young and mature leaves were positively GUS stained, while stems were not (Fig. 9a). In roots, GUS accumulation was observed in branching points where lateral roots are formed and along the primary root being more intense in the tips (Fig. 9b). This finding suggests a role for this kinase in developing roots, such as promoting cellular division and elongation.

In addition, our results show that the promoter is active during different stages of tuber development. When the stolon elongates, intense staining is observed in hooked apical tips (Fig. 9c). In stolons that show incipient swelling, the staining covered all the swollen area, but when radial growth and expansion progressed the staining

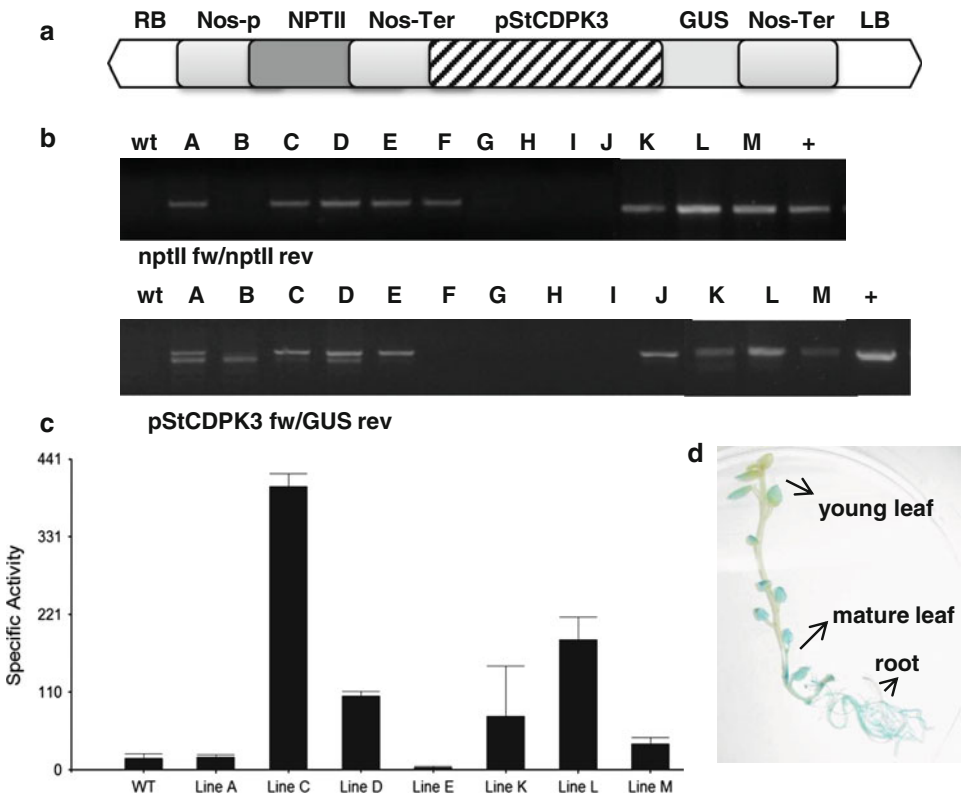

Fig. 8 Transgenic lines carrying pStCDPK3-GUS were obtained. **a** Schematic diagram of the construct pbi101. *RB* right border of T-DNA, Nos-promoter, NPTII selection marker gene, nos-terminator, *LB* left border of T-DNA. **b** Transgene presence was checked by PCR. Genomic DNA from transgenic lines *A*–*M* were used as template and oligonucleotides pairs for nptII gene (Kanamycin resistance) and a fragment including partial sequence of both the StCDPK3 promoter and beta-glucuronidase gene, as indicated. **c** Quantitative MUG (4-methylumbelliferyl-β-D-glucuronide) activity assays were performed using 10 µg of whole plants protein extracts. One unit is defined as the amount of enzyme that hydrolyses 1 µmol/min substrate MUG at 37 °C. The specific activity of GUS was calculated using a calibration curve for MU (4-methylumbelliferone). Three replicates were averaged for each harvest and *error bars* are indicated. **d** GUS stained in vitro grown transgenic potato line C

diminished. Since elongation and swelling both require cytoskeleton reorganization, we propose that StCDPK3 could have a role in cytoskeleton activity. Minitubers from transgenic lines were obtained (5–10 mm) and GUS stained. Promoter activity was detected in meristematic tissues: in the tip of the incipient sprouts and in tuber eyes (Fig. 9d), reinforcing the concept that proliferative growth and elongation mechanisms might require StCDPK3 activity.

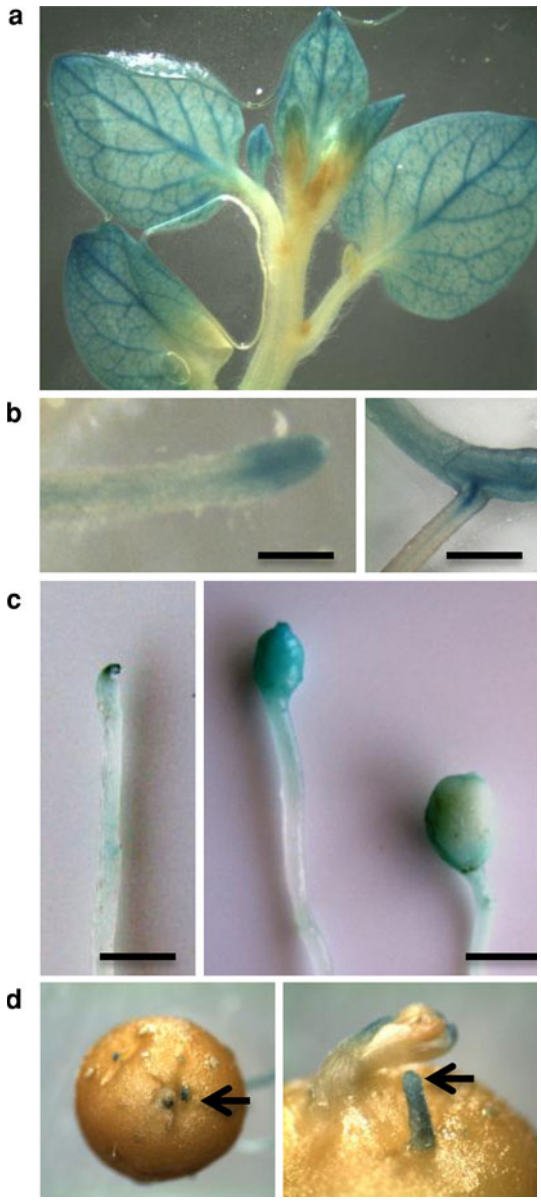

Fig. 9 GUS staining of potato transgenic lines. **a** In vitro grown plants aerial tissues. **b** Root tips and root branching points. **c** Early stolons and swelling stolons. **d** In vitro obtained minitubers. *Arrows* indicate the GUS staining in the minituber eyes and developing etiolated sprouts. *Bar* 2 mm

Discussion

Potato is the third most important crop worldwide so it is important to uncover the mechanism that controls the tuberization and sprouting processes, the two major developmental stages of this plant relevant for agricultural purposes. The interaction of plants with their environment often results in transient calcium increases and it is of particular interest to determine the mechanisms of calcium sensing. Protein kinases are one of the largest groups of calcium sensors, among them CDPKs are able to directly bind calcium ions and modulate their activity. These proteins have been involved in metabolism, in developmental processes, stress responses, and cover different target substrates, indicative of diverse biological roles in plant cells (Klimecka and Muszynska 2007).

In this study, *Stcdpk3* gene was characterized. According to the recently released potato genome sequences, this gene localizes in chromosome 3 consistent with our previous localization assays performed with the SSCP technique. Similar to *Stcdpk1* and *2*, this gene presents the conserved structure of eight exons and seven introns, two of them are particularly long, and further contains an intron in the 5′UTR. Evidence states that natural selection favors short introns in highly expressed genes to minimize the cost of transcription and other molecular processes such as splicing (Castillo-Davis et al. 2002). It was established that introns in highly expressed genes are substantially shorter than those present in genes with low expression, so it is feasible to assume that *StCdpk3* is a low expressed gene. However, there is evidence showing that a 5′UTR intron of the *A. thaliana* EF1α-A3 gene enhanced its expression and that intron size influenced the level of transcription. A deletion series based on the intron length showed that the expression level is dependent either on intron length (the longer the intron, the higher the expression) or on distributed motifs dispersed throughout the 5′ region of the intron (Chung et al. 2006). Intron zero in the 5′UTR of StCDPK3 could as well influence its transcription rate.

The NTV domain of StCDPK3 is characterized by a NORS region rich in proline and glutamine residues. Several transcription factors have been found to contain regions rich in proline or proline/glutamine (Courey and Tjian 1988; Müller et al. 1988; Santoro et al. 1988; Williams et al. 1988). It was proposed that proline/glutamine domains may act as a binding site for recognition and assembly of additional factors during the formation of transcription complexes and spliceosomes (Gerber et al. 1994). In the case of StCDPK3, this region likely mediates protein–protein interactions. Kinase specificity is achieved by the molecular recognition of substrates by catalytic domains (Ito et al. 2011), and differential phosphorylation in the NTV of CDPKs affects their target specificity.

We suggest that the NTV domain of StCDPK3 is important for target identification and interaction, as described for several CDPKs.

The recombinant 6xHisStCDPK3 and 6xHisStCDPK1 proteins were efficiently produced in bacteria and affinity purified. We defined the K_m and V_{max} values for Syntide-2 and ATP of the purified enzymes. StCDPK3 has higher affinity for ATP (K_m 3.3 μM) than StCDPK1 (19.7 μM) or StCDPK2 (K_m 18 μM). The calcium requirements for StCDPK3 kinase and autophosphorylation activities substantially differ from those of StCDPK1 and 2. By displaying different biochemical properties, distinct functions could be assigned to the isoforms, meaning that these kinases are able to decode diverse calcium transients.

It is interesting to mention that StCDPK3 contains a PEST sequence in its NTV domain that could control the protein turnover. A specific antibody against a peptide belonging to the NTV domain of StCDPK3 was generated, but we were unable to detect StCDPK3 protein in tissues such as roots, sprouts, induced stolons and tubers by Western blot, despite the fact that according to our results the kinase is expressed in those tissues. PEST sequences have been associated with rapid protein degradation; their deletion stabilizes a protein that is normally rapidly degraded. This sequence has also been reported in OsCDPK2 from rice and in PnCDPK1 from morning glory (Frattini et al. 1999; Jaworski et al. 2010). OsCDPK2 protein was almost undetectable in rice leaves exposed to light despite the abundant presence of OsCDPK2 mRNA in the mesophyll cells. The authors suggest that the light-induced instability of OsCDPK2 protein may result from the presence of the N-terminal PEST motif (Frattini et al. 1999). We propose that StCDPK3 might follow a similar post-transcriptional mechanism responsible for maintaining low protein levels. In animals, reports state that all PEST proteins are important regulatory molecules and their fast turnover is required for rapid changes in their concentrations, known PEST proteins include oncogene products, key enzymes and components of signal pathways (Rechsteiner 1988).

Transgenic lines carrying the *StCdpk3* promoter fused to GUS presented high activity in root tips and in branching points where lateral root formation starts. Many DNA elements associated with root expression were identified in StCDPK3 promoter sequence. As mentioned, StCDPK3 is highly similar to NtCDPK1 and LeCPK1 (Yoon et al. 1999; Rutschmann et al. 2002) and the three genes share a common expression profile in roots. Down-regulation of *NtCDPK1* transcripts in transgenic tobacco plants resulted in smaller plants showing abnormal root development, with reduced lateral root formation and less elongation (Lee et al. 2006). StCDPK3 could participate in the molecular mechanisms leading to main and lateral roots development, as described for NtCDPK1 (Lee et al. 2006).

CDPKs are known to modulate Ca^{2+}-dependent plant responses caused by phytohormones, mostly gibberellins, cytokinins and auxins (Klimecka and Muszynska 2007). Hormone influences the mRNA levels of CDPKs in the cell, thereby coordinating an appropriate temporal and spatial distribution of these genes in the plant tissues. In tobacco, leaves treatments with ABA and cytokinins resulted in accumulation of *NtCDPK1* transcripts while auxin treatment resulted in much less visible induction (Yoon et al. 1999). *NtCDPK1* and *StCDPK3* display a similar response to ABA, but, while *NtCDPK1* mRNA accumulation is stimulated by GA (Yoon et al. 1999), the phytohormone exerted an inhibitory effect on *StCDPK3* expression. In this way we demonstrate that despite high similarity, different effects are observed between species.

Our results show that *StCDPK3* is expressed in early induced stolons and its expression diminished in advanced tuber formation stages while previous data show that *StCDPK1* is highly expressed in late tuberizing stolons (Raíces et al. 2001). In in vitro grown plants, ABA induced the expression of *StCDPK3*, which is in accordance with the finding of ABRE elements in its promoter, while GA inhibited *StCDPK3* expression. In early stages of tuber formation ABA and sucrose antagonize GA levels in the tip of the stolons committed to tuber formation (Xu et al. 1998), thus the expression of *StCDPK3* could be upregulated in this environment. Then the stolons alter their growth habit displaying a cessation of elongation growth and the initiation of subapical radial growth (Cutter 1978). Increased cell division and expansion is followed rapidly by a massive deposition of starch and storage proteins. The expression of *StCDPK1* is strongly induced by sucrose both in in vitro plants and stolons (Raíces et al. 2003c; Gargantini et al. 2009); therefore sucrose unloading during stolon swelling could promote *StCDPK1* expression in advanced tuberization stages. Cessation of stolon elongation and the onset of stolon swelling require reorganization of the cytoskeleton to reorient the growth pattern in these cells.

The spatial and temporal distribution of CDPK isoforms in plant tissues and organs must be related to specific calcium fluxes. In *Pyrus pyrifolia*, Ca^{2+} activities and fluxes had the same periodicity as pollen germination (Qu et al. 2012). In growing *Limnobium stoloniferum* root hairs, Ca^2 fluxes are localized almost exclusively to the tips and the authors suggested that these fluxes may be involved in directing growth (Jones et al. 1995). A soybean CDPK co-localized with interphase F-actin in *Allium* root cells and *Tradescantia* pollen tubes (Putnam-Evans et al. 1989) suggesting a potential role for CDPKs in the regulation of the plant cytoskeleton, while reports by Zhou et al. (2009) provide a new insight into the potential function of *Arabidopsis* CDPKs in the control of pollen tube polar growth.

Calcium transients in potato stolons and root cells could follow a similar pattern as reported in other species. The spatial localization and transient expression of StCDPK3 in elongating stolons and root tips or branching points suggests that this kinase is tightly controlled both at mRNA and protein level. We suggest that this kinase is responsible for decoding calcium fluxes at these sites, and could then be involved in directing the polarized cell growth pattern by modulating cytoskeleton orientation.

Acknowledgments We thank Salomé Prat Monguío (CSIC, Madrid, Spain) for the cDNA library from tuberizing stolons. RMU is member of CONICET. CG, VG and FS are fellows from CONICET. This work was supported by grants from CONICET (PIP 00037), University of Buenos Aires (UBACYT X225) and FONCYT-ANPCYT (PICT 2005 #32560). Contributions from DH's group were supported by the NSF Plant Genome Research Program award no. DBI-0820659 and National Research Initiative grant no. 2008-02806 from the USDA National Institute of Food and Agriculture Iowa State University (ISU).

References

Asano T, Hakata M, Nakamura H, Aoki N, Komatsu S, Ichikawa H, Hirochika H, Ohsugi R (2011) Functional characterisation of OsCPK21, a calcium-dependent protein kinase that confers salt tolerance in rice. Plant Mol Biol 75:179–191

Asano T, Hayashi N, Kobayashi M, Aoki N, Miyao A, Mitsuhara I, Ichikawa H, Komatsu S, Hirochika H, Kikuchi S, Ohsugi R (2012) A rice calcium-dependent protein kinase OsCPK12 oppositely modulates salt-stress tolerance and blast disease resistance. Plant J. 69:26–36

Balamani V, Veluthambi K, Poovaiah BW (1986) Effect of calcium on tuberization in potato (*Solanum tuberosum* L.). Plant Physiol 80:856–858

Batistic O, Kudla J (2011) Analysis of calcium signaling pathways in plants. Biochim Biophys Acta. doi:10.1016/j.bbagen.2011.10.012

Bonierbale MW, Plaisted RL, Pineda O, Tanksley SD (1994) QTL analysis of trichome-mediated insect resistance in potato. Theor Appl Genet 87:973–987

Castillo-Davis CI, Mekhedov SL, Hartl DL, Koonin EV, Kondrashov FA (2002) Selection for short introns in highly expressed genes. Nat Genet 31:415–418

Chico JM, Raíces M, Tellez-Iñon MT, Ulloa RM (2002) A calcium-dependent protein kinase is systemically induced upon wounding in tomato plants. Plant Physiol 128:256–270

Chung BY, Simons C, Firth AE, Brown CM, Hellens RP (2006) Effect of 5′UTR introns on gene expression in *Arabidopsis thaliana*. BMC Genomics 7:120. doi:10.1186/1471-2164-7-120

Courey AJ, Tjian R (1988) Analysis of Spl in vivo reveals multiple transcriptional domains including a novel glutamine-rich activation motif. Cell 55:887–898

Cutter EG (1978) Structure and development of the potato plant. In: Ivins JD, Milthorpe FL (eds) The Growth of the Potato. Butterworth, London, pp 99–113

Dammann C, Ichida A, Hong B, Romanowsky SM, Hrabak EM, Harmon AC, Pickard BG, Harper JF (2003) Subcellular targeting of nine calcium-dependent protein kinase isoforms from Arabidopsis. Plant Physiol 132:1840–1848

Day IS, Reddy VS, Shad Ali G, Reddy AS (2002) Analysis of EF-hand-containing proteins in Arabidopsis. Genome Biol 3:research0056.1–research0056.24

Dodd AN, Kudla J, Sanders D (2010) The language of calcium signaling. Annu Rev Plant Biol 61:593–620

Feingold S, Lloyd J, Norero N, Bonierbale M, Lorenzen J (2005) Mapping and characterization of new EST-derived microsatellites for potato (*Solanum tuberosum* L.). Theor Appl Genet 111:456–466

Frattini M, Morello L, Breviario D (1999) Rice calcium-dependent protein kinase isoforms OsCDPK2 and OsCDPK11 show different responses to light and different expression patterns during seed development. Plant Mol Biol 41:753–764

Gargantini PR, Gonzalez-Rizzo S, Chinchilla D, Raíces M, Giammaria V, Ulloa RM, Frugier F, Crespi MD (2006) A CDPK isoform participates in the regulation of nodule number in *Medicago truncatula*. Plant J 48:843–856

Gargantini PR, Giammaria V, Grandellis C, Feingold SE, Maldonado S, Ulloa RM (2009) Genomic and functional characterization of StCDPK1. Plant Mol Biol 70:153–172

Geiger D, Scherzer S, Mumm P, Marten I, Ache P, Matschi S, Liese A, Wellmann C, Al-Rasheid KA, Grill E, Romeis T, Hedrich R (2010) Guard cell anion channel SLAC1 is regulated by CDPK protein kinases with distinct Ca^{2+} affinities. Proc Natl Acad Sci USA 107:8023–8028

Gerber HP, Seipel K, Georgiev O, Höfferer M, Hug M, Rusconi S, Schaffner W (1994) Transcriptional activation modulated by homopolymeric glutamine and proline stretches. Science 263:808–811

Giammaria V, Grandellis C, Bachmann S, Gargantini PR, Feingold SE, Bryan G, Ulloa RM (2011) StCDPK2 expression and activity reveal a highly responsive potato calcium-dependent protein kinase involved in light signalling. Planta 233:593–609

Harmon AC (2003) Calcium-regulated protein kinases of plants. Gravit Space Biol Bull 16:83–90

Harper JF, Harmon AC (2005) Plants symbiosis and parasites: a calcium signalling connection. Nat Rev Mol Cell Biol 7:555–566

Ito T, Nakata M, Ishida S, Takahashi Y (2011) The mechanism of substrate recognition of Ca^{2+}-dependent protein kinases. Plant Signal Behav 6:924–926

Jaworski K, Pawełek A, Szmidt-Jaworska A, Kopcewicz J (2010) Expression of calcium-dependent protein kinase gene (PnCDPK1) is affected by various light conditions in pharbitis nil seedlings. J Plant Growth Reg 29:316–327

Jones DL, Shaff JE, Kochian LV (1995) Role of calcium and other ions in directing root hair tip growth in *Limnobium stoloniferum*. Planta 197:672–680

Klimecka M, Muszynska G (2007) Structure and functions of plant calcium-dependent protein kinases. Acta Biochim Pol 54:219–233

Lee SS, Yoon GM, Rho EJ, Moon E, Pai HS (2006) Functional characterization of NtCDPK1 in tobacco. Mol Cells 28:141–146

Mehlmer N, Wurzinger B, Stael S, Hofmann-Rodrigues D, Csaszar E, Pfister B, Bayer R, Teige M (2010) The $Ca^{(2+)}$-dependent protein kinase CPK3 is required for MAPK-independent salt-stress acclimation in Arabidopsis. Plant J 63:484–498

Müller MM, Ruppert S, Schaffner W, Matthias P (1988) A cloned octamer transcription factor stimulates transcription from lymphoid-specific promoters in non-B cells. Nature 8:544–551

Nakata M, Yuasa T, Takahashi Y, Ishida S (2009) CDPK1, a calcium-dependent protein kinase regulates transcriptional activator RSG in response to gibberellins. Plant Signal Behav 4:372–374

Navarro C, Abelenda JA, Cruz-Oró E, Cuéllar CA, Tamaki S, Silva J, Shimamoto K, Prat S (2011) Control of flowering and storage organ formation in potato by FLOWERING LOCUS T. Nature 478:119–122

Putnam-Evans C, Harmon AC, Palevitz BA, Fechheimer M, Milton JC (1989) Calcium-dependent protein kinase is localized with F-actin in plant cells. Cell Motil Cytoskeleton 12:12–22

Qu H, Jiang X, Shi Z, Liu L, Zhang S (2012) Fast loading ester fluorescent Ca^{2+} and pH indicators into pollen of *Pyrus pyrifolia*. J Plant Res 125:185–195

Raíces M, Chico JM, Téllez-Iñón MT, Ulloa RM (2001) Molecular characterization of StCDPK1, a calcium-dependent protein kinase of Solanum tuberosum that is induced at the onset of tuber development. Plant Mol Biol 46:591–601

Raíces M, MacIntosh GC, Ulloa RM, Gargantini PR, Vozza NF, Téllez-Iñón MT (2003a) Sucrose increases calcium-dependent protein kinase and phosphatase activities in potato plants. Cell Mol Biol 49:959–964

Raíces M, Gargantini PR, Chinchilla D, Crespi M, Tellez-Iñon MT, Ulloa RM (2003b) Regulation of CDPK isoforms during tuber development. Plant Mol Biol 52:1011–1024

Raíces M, Ulloa RM, MacIntosh G, Crespi MD, Téllez-Iñón MT (2003c) StCDPK1 is expressed in potato stolon tips and is induced by high sucrose concentration. J Exp Botany 54:2589–2591

Rechsteiner M (1988) Regulation of enzyme levels by proteolysis: the role of pest regions. Adv Enzyme Regul 27:135–151

Romeis T, Piedras P, Jones JDG (2000) Resistance gene dependent activation of a calcium-dependent protein kinase in the plant defense response. Plant Cell 12:803–815

Rutschmann F, Stalder U, Piotrowski M, Oecking C, Schaller A (2002) LeCPK1, a calcium-dependent protein kinase from tomato. Plasma membrane targeting and biochemical characterization. Plant Physiol 129:156–168

Santoro C, Mermod N, Andrews PC, Tjian R (1988) A family of human CCAAT-box-binding proteins active in transcription and DNA replication: cloning and expression of multiple cDNAs. Nature 334:218–224

Schlessinger A, Punta M, Rost B (2007) Natively unstructured regions in proteins identified from contact predictions. Bioinformatics 23:2376–2384

Wheeler GL, Brownlee C (2008) Ca^{2+} signalling in plants and green algae: changing channels. Trends Plant Sci 13:506–514

Williams T, Admon A, Lüscher B, Tjian R (1988) Cloning and expression of AP-2, a cell-type-specific transcription factor that activates inducible enhancer elements. Genes Dev 2: 1557–1569

Witte CP, Keinath N, Dubiella U, Demoulière R, Seal A, Romeis T (2010) Tobacco calcium-dependent protein kinases are differentially phosphorylated in vivo as part of a kinase cascade that regulates stress response. J Biol Chem 285:9740–9748

Wurzinger B, Mair A, Pfister B, Teige M (2011) Cross-talk of calcium-dependent protein kinase and MAP kinase signaling. Plant Signal Behav 6:8–12

Xu X, van Lammeren AA, Vermeer E, Vreugdenhil D (1998) The role of gibberellin abscisic acid and sucrose in the regulation of potato tuber formation in vitro. Plant Physiol 117:575–584

Ye S, Wang L, Xie W, Wan B, Li X, Lin Y (2009) Expression profile of calcium-dependent protein kinase (CDPKs) genes during the whole lifespan and under phytohormone treatment conditions in rice (*Oryza sativa* L. ssp. indica). Plant Mol Biol 70:311–325

Yoon GM, Cho HS, Ha HJ, Liu JR, Lee HP (1999) Characterization of NtCDPK1, a calcium-dependent protein kinase gene in Nicotiana tabacum and the activity of its encoded protein. Plant Mol Biol 39:991–1001

Zhou L, Fu Y, Yang Z (2009) A genome-wide functional characterization of arabidopsis regulatory calcium sensors in pollen tubes liming. J Integr Plant Biol 51:751–761